Comment on “Chirality-Induced Electron Spin Polarization and Enantiospecific Response in Solid-State Cross-Polarization Nuclear Magnetic Resonance”

Amrit Venkatesh,[1] Anuradha V. Wijesekara,[1] Luke A. O’Dell,[2]* Aaron J. Rossini[1]*

[1]Iowa State University, Department of Chemistry, Ames, IA, USA, 50011
[2]Institute for Frontier Materials, Deakin University, Geelong, Victoria 3220, Australia
*Authors to whom correspondence should be addressed:
Aaron J. Rossini, arossini@iastate.edu
Luke A. O’Dell, luke.odell@deakin.edu.au

Recently, Santos *et al.* published an article titled “Chirality-Induced Electron Spin Polarization and Enantiospecific Response in Solid-State Cross-Polarization Nuclear Magnetic Resonance” in *ACS Nano*.[1] In this article it was claimed that crystalline amino acid enantiomers can give rise to ^{1}H-^{15}N and ^{1}H-^{13}C cross-polarization magic angle spinning (CPMAS) solid-state NMR spectra with different relative signal intensities. The authors attributed such differences to transient changes in T_1 relaxation times resulting from an interaction between the electron spins and the radiofrequency contact pulses used in the CPMAS experiment, and discussed this proposed phenomenon in terms of the chirality-induced spin selectivity (CISS) effect.

We disagree with the authors conclusion that the CISS effect plays a role in the different signal intensities observed in the CPMAS solid-state NMR spectra of crystalline enantiomers. Putting aside any fundamental arguments about how radiofrequency electromagnetic fields might interact with electron spins in diamagnetic solids at typical NMR magnetic field strengths, or how slight chirality induced differences in electron spin polarization could affect the intensity of CPMAS NMR signals, the most straightforward explanation for the reported differences in CPMAS signal intensities of enantiomers is that the enantiomers exhibit distinct proton longitudinal relaxation times (T_1(^{1}H)). It is a well-known phenomenon in solid-state NMR spectroscopy that the T_1 of abundant, high-gyromagnetic ratio (ɣ) nuclei such as ^{1}H and ^{19}F is highly dependent upon sample purity, crystallinity and particle size. For example, Bloembergen showed in 1949 that ^{19}F longitudinal relaxation in CaF_2 was largely driven by paramagnetic iron dopants, with T_1(^{19}F) showing a variation of over three orders of magnitude depending upon the concentration of iron in the CaF_2 samples.[2] Rabbani and Edmonds showed that milling can significantly reduce T_1(^{1}H) in solids.[3] They hypothesized that the reduction in T_1(^{1}H) was due to the combination of rapid relaxation of surface defects and ^{1}H spin diffusion which homogenizes the magnetization over the sample.[3] Munson and co-workers also showed that grinding/milling can lead to a large reduction in T_1(^{1}H) for different organic solids.[4-6] Hu and co-workers recently demonstrated that extensive ball-milling can reduce T_1(^{1}H) by one to two order of magnitude for microcrystalline solids with intrinsic T_1(^{1}H) on the order of thousands of seconds.[7] Presumably, grinding leads to the formation of amorphous domains, crystalline vacancies, surface defects and/or paramagnetic impurities that cause a reduction in T_1(^{1}H).[3-7] Despite the fact that the paramagnetic dopants or defects may be dilute or restricted to surfaces, rapid homonuclear spin diffusion often leads to observation of a mono-exponential T_1 in the solid-state for ^{1}H and ^{19}F.[2,4-7] It should also be noted that solids possessing methyl groups, ammonium groups and waters of hydration sometimes have short T_1(^{1}H) on the order of a few seconds. The short T_1(^{1}H) arises because these functional groups often undergo fast dynamic reorientation with correlation times near the inverse of the ^{1}H Larmor frequency.[8,9] In solids where T_1(^{1}H) is short because of dynamic functional groups, T_1(^{1}H) is likely to be less sensitive to the presence of impurities/defects and sample preparation.

To illustrate that the variations in ^{13}C CPMAS signal intensity observed by Santos *et al.* for the different enantiomers are likely caused by standard differences in T_1(^{1}H) that are unrelated to the CISS effect or the particulars of the CPMAS pulse sequence, we have performed ^{1}H saturation recovery measurements and ^{1}H-^{13}C CPMAS experiments on D-aspartic acid and L-aspartic acid. Aspartic acid was chosen because Santos *et al.* reported that aspartic acid showed the largest difference in D and L enantiomer ^{15}N and ^{13}C CPMAS signal intensities out of all the amino acids they examined (the D enantiomer ^{15}N CPMAS signal showed a peak area 2.2 times greater than the L enantiomer signal).[1] We also performed NMR experiments on both enantiomers of aspartic acid after recrystallization from a saturated aqueous solution.

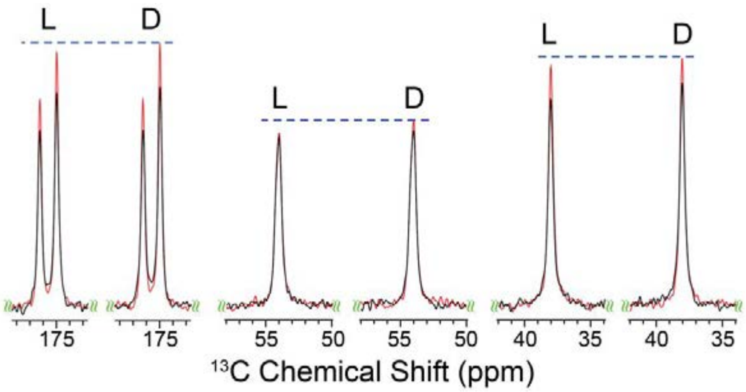

Figure 1. Comparison of isotropic peak intensities in natural isotopic abundance ^{13}C CPMAS NMR spectra of as received L- and D-aspartic acid (red traces) and recrystallized samples (black traces). Horizontal dashed lines are guides for the eye to facilitate peak intensity comparison. All spectra were obtained with a CP-spin echo pulse sequence, an 8 kHz MAS frequency, a 500 µs CP contact time, 100 kHz SPINAL-64 ^{1}H heteronuclear decoupling and 8 scans. The recycle delay for each spectrum and the relative integrated intensity of each peak is indicated in Table 1.

Table 1. Summary of Saturation Recovery and ^{1}H-^{13}C CPMAS Experiments on D-Aspartic Acid and L-Aspartic Acid.

			Relative Integrated Intensity			
Sample	$T_1(^1\text{H})$ (s)^a	Recycle Delay (s)	176.3 ppm	174.9 ppm	54.0 ppm	38.0 ppm
D-Asp	37(2)	200	1.00	1.29	1.49	1.64
L-Asp	55(1)	300	1.06	1.34	1.45	1.63
D-Asp Recrystallized	20(1)	105	1.09	1.28	1.51	1.66
L-Asp Recrystallized	27(1)	150	1.03	1.24	1.41	1.63

$^aT_1(^1\text{H})$ was measured by individually fitting the intensity of the four isotropic ^{13}C NMR signals as a function of the saturation recovery delay. The indicated $T_1(^1\text{H})$ was the average of the values measured for the build-up of the four isotropic ^{13}C NMR signals. The standard deviation is given in parentheses.

Figure 1 and Table 1 summarize the results of the ^{1}H-^{13}C CPMAS experiments on the different aspartic acid samples. First, T_1(^{1}H) was measured for each sample with a ^{13}C CPMAS detected ^{1}H saturation recovery experiment. T_1(^{1}H) was determined by recording the ^{13}C CPMAS NMR signal as a function of the saturation delay (τ) and fitting the signal intensities to a standard mono-exponential saturation recovery function:

$$S(\tau) = S_0\left[1 - \exp(-\tau / T_1)\right]$$

where S_0 is the fitted equilibrium signal intensity. Note that the same values of T_1(^{1}H) would be measured if a ^{1}H detected saturation recovery experiment was used. The measured values of T_1(^{1}H) are given in Table 1. T_1(^{1}H) of 37 s and 55 s were measured for the as-received, unground samples of D-aspartic acid and L-aspartic acid, respectively. T_1(^{1}H) decreased to 20 s and 27 s for the recrystallized and lightly ground samples of D-aspartic acid and L-aspartic acid, respectively. The reduction in T_1(^{1}H) could be due to trace paramagnetic metal ions present in the deionized water used for recrystallization or sample grinding. Regardless, the large range in the measured T_1(^{1}H) for the different aspartic acid samples illustrates that the dependence of T_1(^{1}H) upon the sample preparation, consistent with numerous prior solid-state NMR experiments.[2-7] Note that such large variations in relaxation times would completely dominate over any minor or "transient" variations caused by the CISS-related phenomena proposed by Santos *et al.*, and would have to be fully accounted for before such phenomena could be quantified.

With knowledge of T_1(^{1}H) for each sample, quantitative ^{13}C CPMAS of the different aspartic acid samples were acquired with a recycle delay of more than 5 × T_1(^{1}H) to ensure complete longitudinal relaxation. There are some slight variations in peak intensity (height) visible in Figure 1, which arise because of slight differences in peak widths. The variation in peak width could reflect differences in the crystallinity of the samples. As expected, comparison of the relative integrated intensity for each peak shows extremely minor differences that are within experimental error and could be accounted for by trivial factors such as sample purity (we note that commercially available amino acid enantiomers usually differ in their advertised purity by several percent).

Santos *et al.* observed that the ^{15}N and ^{13}C CPMAS signal intensity (peak area) of as received D-aspartic acid was 2.2 times greater than that of L-aspartic acid when a 20 s recycle delay was employed.[1] Critically, they did not measure T_1(^{1}H) for either sample, therefore it is likely that any differences in CPMAS signal intensity can be attributed solely to saturation/incomplete relaxation, especially if the recycle delays were less than T_1(^{1}H). For example, if their samples of L-aspartic acid had a T_1(^{1}H) of 55 s and D-aspartic acid had a T_1(^{1}H) of 20 s, then CPMAS experiments obtained with a 20 s recycle delay would show about a factor two difference in signal intensities. Indeed, Santos *et al.* reported that the ^{15}N CPMAS spectra of the two aspartic acid enantiomers obtained with a much shorter recycle delay of 1 s shows no signal from L-aspartic acid,[1] possibly suggesting that the L-aspartic acid has a longer T_1(^{1}H) than D-aspartic acid.

Several other observations bring the conclusions of Santos *et al.* into doubt. The differences in the D- and L-isomer ^{13}C and ^{15}N CPMAS signal intensities were very small for several of the amino acids they examined and are likely within the experimental uncertainties (*e.g.*, signal intensity ratios on the order of 0.9/1.1).[1] This observation could be explained by the fact that the CPMAS signal intensities will be similar if the amino acids have a comparable T_1(^{1}H) for different enantiomers. Finally, we note that many of the ^{15}N CPMAS spectra they presented had a low signal to noise ratio which makes it difficult to accurately compare peak intensities and areas.[1]

Considering the data presented here and the arguments outlined above, we believe that the variation in CPMAS signal intensities reported by Santos *et al.* do not arise from chirality induced effects, rather they can be attributed solely to ordinary variations in T_1(^{1}H) and the acquisition of NMR spectra with recycle delays of less than $3 \times T_1$(^{1}H) of the slowest relaxing enantiomer. These differences in T_1(^{1}H) for the different enantiomers likely arise because of slight differences in sample purity, particle size and crystallinity as has been well documented in the literature[2-7] and is illustrated by NMR experiments on aspartic acid performed here.

Experimental

L-aspartic acid (BioUltra grade) and D-aspartic acid (ReagentPlus grade) were purchased from Sigma Aldrich and used as received. L- and D-aspartic acid were also recrystallized from a saturated deionized water solution using a slow evaporation technique. After approximately 50%

of the solution had evaporated over several days, the precipitated microcrystals were collected on filter paper, washed with water, dried in an oven for 30 minutes at 80° C, then lightly ground by hand and transferred to the rotor. The observed isotropic ^{13}C chemical shifts were identical before and after recrystallization, confirming that there was no change in crystalline form.

All solid-state NMR experiments were performed with a widebore 9.4 T NMR spectrometer equipped with a Bruker Avance III HD console and a 4.0 mm HX probe. Samples were center-packed into the central 1/3rd of the rotor by packing polytetrafluoroethylene powder into the outer ends of the rotor. Center-packed samples were used to improve quantification by reducing radiofrequency inhomogeneity effects and ensuring that all of the sample in the rotor contributes to the detected NMR signal. For all quantitative NMR experiments 40 mg ± 1 mg of material were packed into a 4 mm rotor. The MAS rate was set to 8 kHz. The ^{13}C and ^{1}H CP spin-lock rf fields were approximately 48 kHz and 56 kHz, respectively, to satisfy the MAS modified Hartmann-Hahn match condition. The amplitude of the ^{1}H spin-lock pulse rf field was linearly ramped to broaden the Hartmann-Hahn match condition.[10] The CP contact time was 500 μs. SPINAL-64 heteronuclear decoupling was applied with a ^{1}H RF field of 100 kHz.[11] $T_1(^{1}H)$ was measured using a $^{1}H \rightarrow ^{13}C$ CP-saturation recovery pulse sequence (^{1}H saturation – ^{1}H longitudinal relaxation for time τ – $^{1}H \rightarrow ^{13}C$ CP – ^{13}C NMR signal detection). ^{1}H saturation was performed with a comb of ^{1}H $\pi/2$ pulses and a dummy scan. Quantitative 1D $^{1}H \rightarrow ^{13}C$ CPMAS solid-state NMR spectra were obtained with a rotor-synchronized CP-spin echo pulse sequence (CP – τ_{rot} – π – τ_{rot} – acquire) to eliminate receiver dead time effects. Each spectrum was obtained with 8 scans and a recycle delay greater than 5× $T_1(^{1}H)$.

Acknowledgements

This material is based upon work supported by the National Science Foundation under Grant No. 1709972 to AJR.

References:

(1) Santos, J. I.; Rivilla, I.; Cossío, F. P.; Matxain, J. M.; Grzelczak, M.; Mazinani, S. K. S.; Ugalde, J. M.; Mujica, V. Chirality-Induced Electron Spin Polarization and Enantiospecific Response in Solid-State Cross-Polarization Nuclear Magnetic Resonance. *ACS Nano* **2018**, *12*, 11426-11433.
(2) Bloembergen, N. On the Interaction of Nuclear Spins in a Crystalline Lattice. *Physica* **1949**, *15*, 386-426.
(3) Rabbani, S. R.; Edmonds, D. T. Nuclear Spin-Lattice Relaxation-Time Reduction in Small Particles. *Phys. Rev. B* **1994**, *50*, 6184-6188.
(4) Lubach, J. W.; Xu, D.; Segmuller, B. E.; Munson, E. J. Investigation of the Effects of Pharmaceutical Processing Upon Solid-State NMR Relaxation Times and Implications to Solid-State Formulation Stability. *J. Pharm. Sci.* **2007**, *96*, 777-787.
(5) Dempah, K. E.; Barich, D. H.; Kaushal, A. M.; Zong, Z.; Desai, S. D.; Suryanarayanan, R.; Kirsch, L.; Munson, E. J. Investigating Gabapentin Polymorphism Using Solid-State NMR Spectroscopy. *AAPS PharmSciTech* **2013**, *14*, 19-28.
(6) Dempah, K. E.; Lubach, J. W.; Munson, E. J. Characterization of the Particle Size and Polydispersity of Dicumarol Using Solid-State NMR Spectroscopy. *Mol. Pharm.* **2017**, *14*, 856-865.
(7) Lou, X.; Shen, M.; Li, C.; Chen, Q.; Hu, B. Reduction of the 13C Cross-Polarization Experimental Time for Pharmaceutical Samples with Long T1 by Ball Milling in Solid-State NMR. *Solid State Nucl. Magn. Reson.* **2018**, *94*, 20-25.
(8) Stejskal, E. O.; Gutowsky, H. S. Proton Magnetic Resonance of the CH3 Group. Iv. Calculation of the Tunneling Frequency and of T1 in Solids. *J. Chem. Phys.* **1958**, *28*, 388-396.
(9) Allen, P. S.; Clough, S. Tunneling-Assisted Nuclear Spin-Lattice Relaxation. *Phys. Rev. Lett.* **1969**, *22*, 1351-1353.
(10) Peersen, O.; Wu, X.; Kustanovich, I.; Smith, S. Variable-Amplitude Cross-Polarization MAS NMR. *J. Magn. Reson., Ser A* **1993**, *104*, 334-339.
(11) Fung, B. M.; Khitrin, A. K.; Ermolaev, K. An Improved Broadband Decoupling Sequence for Liquid Crystals and Solids. *J. Magn. Reson.* **2000**, *142*, 97-101.